Growth of Organic Crystalline Thin Films with Strong Second-Order Nonlinearity for Integrated Optics

Artur Hermans[1,2], Stéphane Clemmen[1,2,3], Roel Baets[1,2], Jan Genoe[4,5], Cédric Rolin[4]
[1] Photonics Research Group, Ghent University-imec, 9052 Ghent, Belgium
[2] Center for Nano- and Biophotonics, Ghent University, 9052 Ghent, Belgium
[3] Laboratoire d'Information Quantique, Université Libre de Bruxelles, 1050 Brussels, Belgium
[4] Large Area Electronics Department (LAE), imec, 3001 Leuven, Belgium
[5] Department of Electrical Engineering (ESAT), KU Leuven, 3001 Leuven, Belgium
e-mail: Artur.Hermans@UGent.be

ABSTRACT

We demonstrate the growth of highly nonlinear crystalline thin films of *N*-benzyl-2-methyl-4-nitroaniline (BNA) with a controllable crystal orientation. These films are obtained by crystallizing the material in a temperature gradient. Through second-harmonic generation experiments at a fundamental wavelength of 1550 nm, we found a second-order nonlinearity of (153 ± 70) pm/V. This greatly exceeds the value of 54 pm/V for $LiNbO_3$, the benchmark nonlinear crystal. Moreover, the crystalline films are grown on amorphous substrates with processing temperatures not exceeding 115°C, making them suitable for back-end photonic integration on a CMOS chip. We envisage the growth of BNA crystalline films on silicon nitride photonic integrated circuits, where a strong second-order nonlinearity is lacking.

Keywords: nonlinear materials, thin films, crystal growth, organic crystals, second-harmonic generation

1. INTRODUCTION

A whole range of optical devices relies on second-order nonlinear optical processes. Prime examples include optical parametric oscillators (OPO's) [1] and high-speed electro-optic modulators [2]. Commercial devices tend to be bulky, expensive and power-hungry. Integrating them on a photonic chip would reduce their footprint and increase their energy efficiency. Moreover, once a high-yield mass fabrication process is established, the cost per device goes down drastically.

Dedicated material platforms such as AlGaAs [3] and $LiNbO_3$ on insulator [4] are being developed. These can offer low-loss propagation and a large second-order nonlinearity (also known as second-order susceptibility $\chi^{(2)}$). But, when it comes to high-volume fabrication, silicon (Si) photonics is the technology of choice. Within Si photonics, silicon-on-insulator is the main material platform, but silicon nitride (SiN) is gaining ground as an alternative low-loss platform with a transparency window covering visible wavelengths [5]. Furthermore, SiN can be deposited at low temperatures (< 400°C) through PECVD (Plasma-Enhanced Chemical Vapor Deposition), which allows for back-end photonic integration on CMOS electronics [6]. Unfortunately, the $\chi^{(2)}$ nonlinearity of Si, amorphous SiO_2 and SiN is expected to vanish due to their centrosymmetric nature. Yet, there have been demonstrations of $\chi^{(2)}$ effects in Si [7] and SiN [8], but the exact origin remains elusive and the nonlinearities modest. Therefore, many research efforts focus on combining Si photonics with $\chi^{(2)}$ materials.

One such class of materials are the ferroelectric materials (e.g. $BaTiO_3$, $LiNbO_3$, PZT), which typically exhibit a strong Pockels effect. This makes them particularly interesting for electro-optic modulation. High-speed modulators have been demonstrated by growing epitaxial $BaTiO_3$ on Si [9] and depositing PZT (lead zirconate titanate) thin films on SiN waveguides [2].

Next to these ferroelectric materials, organic $\chi^{(2)}$ materials have received considerable attention in the context of photonic integration. Organic materials can have very large $\chi^{(2)}$ nonlinearities. Their linear and nonlinear polarizability is typically mostly electronic in origin, as opposed to inorganic ferroelectric materials, which tend to have large contributions from ionic movements [10]. Hence, the $\chi^{(2)}$ nonlinearity and permittivity of those organic materials varies little up to the near-infrared to visible frequency range. These properties make organic $\chi^{(2)}$ materials extremely interesting both for (very) high-speed modulators and nonlinear wave mixing applications. Moreover, organic $\chi^{(2)}$ materials can be processed at low temperatures, making them suitable for back-end integration on a CMOS chip. Highly efficient modulators have been realized by covering Si slot waveguides with randomly ordered organic nonlinear molecules [11]. To get a large effective $\chi^{(2)}$, the molecules need to be aligned by poling the material. Alternatively, one can make use of organic $\chi^{(2)}$ crystals which do not

The research leading to these results has received funding from the European Research Council (ERC) under the EU's Horizon 2020 research and innovation programme (grant agreement n°742299 / Video Holography). A. H. thanks FWO for funding. S. C. acknowledges the financial support of the F.R.S.-FNRS.

require poling, since the molecules are already ordered in a crystalline structure [12]. Nonetheless, growing crystalline thin films on a photonic integrated circuit (PIC) is challenging.

A well-known organic nonlinear crystal is BNA (*N*-benzyl-2-methyl-4-nitroaniline). Its nonlinearity has been determined in bulk crystals (orthorhombic crystal system, point group mm2) through second-harmonic generation (SHG) experiments at a fundamental wavelength of 1064 nm [12]. The largest nonlinear tensor element χ_{zzz} was found to be (468 ± 62) pm/V, compared to χ_{zzz} = 54 pm/V for $LiNbO_3$ [13]. Next to having a large nonlinearity, BNA is transparent in the ~500 nm to ~2 µm wavelength range and stable in water [12]. The growth of BNA crystals has already been demonstrated in silicon slot waveguides [14]-[15], where molten BNA was used to fill up slots through capillary flow before crystallizing the material. However, this approach offers little freedom in terms of device design. Ideally, one would be able to grow single crystals in thin films over large areas. In combination with photolithographic processing, this would open up numerous possibilities for the realization of highly efficient integrated $\chi^{(2)}$ devices.

Here, we demonstrate the growth of highly nonlinear crystalline thin films of BNA with a controllable crystal orientation. The crystals are grown on amorphous substrates with processing temperatures not exceeding 115°C. This makes BNA suitable for integration on SiN PIC's and allows for back-end integration on a CMOS chip.

2. FABRICATION

We use 2 cm x 2 cm glass substrates and Si substrates with 3 µm wet oxide. After cleaning, we drop cast 100 µl of 0.4 wt% BNA in toluene solution on a glass or Si substrate. After the solvent has evaporated, we place an FDTS (perfluorodecyltrichlorosilane) treated glass cover on top. The glass cover is needed to avoid dewetting during melting. We treat the cover with FDTS to prevent sticking when we remove the cover for characterization. Next, the sample is placed on a hotplate for several minutes to melt the BNA (BNA melts at 105°C [15]) and removed again to let it crystallize at room temperature, resulting in a polycrystalline BNA film. To grow large single crystals of BNA, we move this polycrystalline film through a temperature gradient [16]. This is done with a homebuilt tool consisting of two hotplates: one set to 115°C and the other to 65°C. There is a gap of 2 mm between the hotplates. Using a stepper motor, the sample is slid from the hot to the cold stage at a speed of 0.7 µm/s. When placing the sample on our tool, we ensure that part of the sample starts out on the cold stage. This way, the polycrystalline BNA film acts as a seed. Also, for Si substrates, we place the sample on the tool with the Si facing up, to avoid creating a thermal bridge. Figure 1a shows an image of a sample on our tool, with clearly visible crystals. The glass cover is removed before characterization of the films.

3. CHARACTERIZATION

Apart from visual inspection with a microscope, the samples are characterized by x-ray diffraction (XRD) θ-2θ scans and SHG experiments. For the SHG experiments, we use a laser emitting 100 fs pulses at a wavelength of 1550 nm. The laser light is linearly polarized and the electric field direction is altered with a half-wave plate. The laser beam is perpendicularly incident onto the sample and the measurements are conducted in transmission. Before detection, the transmitted laser light is filtered out such that only the SH light remains. Also, a polarizer is present in front of the detector to select the polarization of interest. More details about the setup can be found in [17]. The SHG setup is calibrated with a BBO crystal. A transfer matrix model is used to fit the data [18].

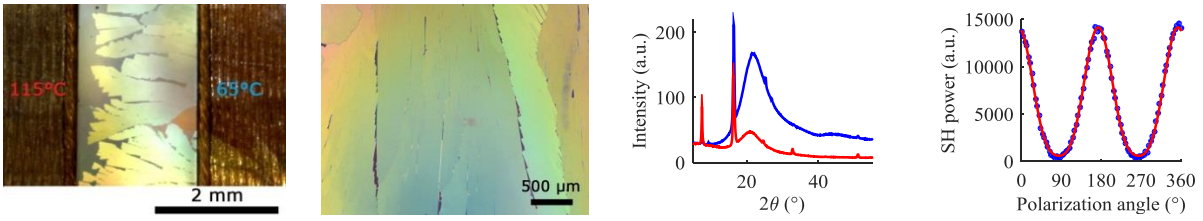

(a) (b) (c) (d)

Figure 1. (a) Image of sample (glass substrate) on the thermal gradient tool. In the gap between the hotplates you can see growing crystals. (b) Differential interference contrast microscopy image of BNA grown on oxidized Si. The crystals grew from the top to the bottom of the image. (c) XRD θ-2θ scan (using Cu Kα radiation) of BNA grown on glass (blue) and on oxidized Si (red). (d) Power of generated second-harmonic light measured as a function of the electric field direction of the incident laser beam (for normal incidence). Blue dots are the measurement data; red line is the fitted curve. 0° corresponds to an electric field perpendicular to the optical table. The BNA crystals are oriented with their long side (direction // temperature gradient) perpendicular to the table; the transmission axis of the polarizer in front of the detector has the same orientation.

Figure 1b shows a microscopy image of BNA crystals grown on oxidized Si. The crystals grew from the top to the bottom of the image. We observe crystals that are several millimeters long and hundreds of micrometers wide. Some cracks and gaps in and in between the crystals are visible.

Figure 1c shows the XRD θ-2θ scans for BNA crystals grown on glass (blue) and oxidized Si substrates (red). Distinct peaks are visible at 8° and 16° and smaller ones at 25°, 33° and 51°. These correspond to the

higher-order diffraction peaks of BNA's (010) plane [14], though the peak at 33° also has a contribution from the Si 200 reflection. The broad peak around 21° is originating from the substrate.

Film thicknesses were measured with a surface profilometer. We observe thicknesses from 100 nm to 700 nm. Better thickness control might be achieved using alternative deposition methods like spin coating or vapor phase deposition techniques.

Knowing the out-of-plane crystal axis (from XRD), the thickness and refractive index [12], the nonlinearity can be estimated from SHG measurements. A typical measurement is shown in Fig. 1d. For BNA on glass substrates we found $\chi_{zzz} = (153 \pm 70)$ pm/V, where the large error is due to thickness uncertainty. This is close to the value of ~160 pm/V at 1550 nm reported in [19] for a bulk crystal. We also detected SHG for BNA on oxidized Si, but the roughness of the unpolished backside made $\chi^{(2)}$ quantification difficult. Our SHG measurements indicate that the crystals have a preferential in-plane orientation, with their Z- or c-axis being parallel to the temperature gradient direction (= pulling direction).

4. CONCLUSIONS

We demonstrated the growth of crystalline BNA thin films with a controllable crystal orientation on amorphous substrates utilizing a temperature gradient crystallization technique. SHG measurements indicate that the crystals grow with their Z- or c-axis along the temperature gradient direction. The nonlinear tensor element χ_{zzz} was determined to be (153 ± 70) pm/V at a fundamental wavelength of 1550 nm. Considering the crystal orientation, χ_{zzz} can be probed using waveguide TE modes and in-plane RF electric fields for modulation. Future works include the growth of BNA crystals on SiN waveguides and loss characterization.

REFERENCES

[1] J.A. Giordmaine, R.C. Miller: Tunable coherent parametric oscillation in $LiNbO_3$ at optical frequencies, *Phys. Rev. Lett.*, 14, 973, 1965.

[2] K. Alexander, *et al.*: Nanophotonic Pockels modulators on a silicon nitride platform, *Nat. Commun.*, 9, 3444, 2018.

[3] L. Ottoviano, *et al.*: Low-loss high-confinement waveguides and microring resonators in AlGaAs-on-insulator, *Opt. Lett.*, 41, 3996, 2016.

[4] C. Wang, *et al.*: Integrated lithium niobate electro-optic modulators operating at CMOS-compatible voltages, *Nature*, 562, 101, 2018.

[5] A. Rahim, *et al.*: Expanding the silicon photonics portfolio with silicon nitride photonic integrated circuits, *J. Lightwave Technol.*, 35, 639, 2017.

[6] Y.H.D. Lee, M. Lipson: Back-end deposited silicon photonics for monolithic integration on CMOS, *IEEE J. Sel. Top. Quantum Electron*., 19, 8200207, 2013.

[7] R.S. Jacobsen, *et al.*: Strained silicon as a new electro-optic material, *Nature*, 441, 199, 2006.

[8] T. Ning, *et al.*: Strong second-harmonic generation in silicon nitride films, *Appl. Phys. Lett.*, 100, 161902, 2012.

[9] C. Xiong, *et al.*: Active silicon integrated nanophotonics: ferroelectric $BaTiO_3$, *Nano Lett.*, 14, 1419, 2014.

[10] M. Jazbinsek, L. Mutter, P. Günter: Photonic applications with the organic nonlinear optical crystal DAST, *IEEE J. Sel. Top. Quantum Electron*., 14, 1298, 2008.

[11] C. Koos, *et al.*: Silicon-organic hybrid (SOH) and plasmonic-organic hybrid (POH) integration, *J. Lightwave Technol.*, 34, 256, 2016.

[12] M. Fujiwara, *et al.*: Determination of the *d*-tensor components of a single crystal of *N*-benzyl-2-methyl-4-nitroaniline, *Jpn. J. Appl. Phys.*, 46, 1528, 2007.

[13] D. A. Roberts: Simplified characterization of uniaxial and biaxial nonlinear optical crystals: a plea for standardization of nomenclature and conventions, *IEEE J. Quantum Electron.*, 28, 2057, 1992.

[14] H. Figi, *et al.*: Electro-optic modulation in horizontally slotted silicon/organic crystal hybrid devices, *J. Opt. Soc. Am. B*, 28, 2291, 2011.

[15] D. Korn, *et al.*: Electro-optic organic crystal silicon high-speed modulator, *IEEE Photon. J.*, 6, 2700109, 2014.

[16] G. Schweicher, *et al.:* Toward single crystal thin films of terthiophene by directional crystallization using a thermal gradient, *Cryst. Growth Des.*, 11, 3663, 2011.

[17] A. Hermans, *et al.*: Growth of thin film organic crystals with strong nonlinearity for on-chip second-order nonlinear optics, *Symposium IEEE Photonics Society Benelux*, Brussels, Belgium, November 2018, p. 55.

[18] D.S. Bethune: Optical harmonic generation and mixing in multilayer media: extension of optical transfer matrix approach to include anisotropic materials, *J. Opt. Soc. Am. B*, vol. 8, 367, 1991.

[19] T. Notake, *et al.*: Ultra-precise processing and Maker fringe measurements of organic N-Benzyl-2-Methyl-4-Nitroaniline crystal, *IRMMW-THz*, Nagoya, Japan, September 2018.